

Feasibility study of wide-band low-profile ultrasonic sensor with flexible piezoelectric paint

Xin Li

Department of Civil & Environmental Engineering, Lehigh University, Bethlehem, PA 18015, USA

Yunfeng Zhang*

Department of Civil & Environmental Engineering, University of Maryland, College Park, MD 20742, USA

(Received March 28, 2007, Accepted December 14, 2007)

Abstract. This paper presents a feasibility study of flexible piezoelectric paint for use in wide-band low-profile surface-mount or embeddable ultrasonic sensor for *in situ* structural health monitoring. Piezoelectric paint is a piezoelectric composite with 0-3 connectivity. Because of its ease of application, piezoelectric paint can be readily fabricated into sensing element with complex pattern. This study examines the characteristics of piezoelectric paint in acoustic emission signal and ultrasonic guided wave sensing. A series of ultrasonic tests including pitch catch and pencil break tests were performed to validate the ultrasonic wave sensing capability of piezoelectric paint. The results of finite element simulation of ultrasonic wave propagation, and acoustic emission generated by a pencil lead break on an aluminum plate are also presented in this paper along with corresponding experimental data. Based on the preliminary experimental results, the piezoelectric paint appears to offer a promising sensing material for use in real-time monitoring of crack initiation and propagation in both metallic and composite structures.

Keywords: acoustic emission; crack; nondestructive evaluation; piezoelectricity; sensor; ultrasonic.

1. Introduction

Piezoelectric materials can be broadly classified into three major categories (Ikeda 1990): ferroelectric ceramics, piezoelectric polymers, and piezoelectric composites. Because of their electro-mechanical coupling property, piezoelectric materials have been widely used for sensing and actuation applications (e.g. Polla and Francis 1998, Damjanovic, *et al.* 2001, Niezrecki, *et al.* 2001, Gautschi 2002). Piezoelectric materials have been used as surface-mount sensors to measure physical movement or strain by directly bonding or embedding piezoelectric thin sheets onto the structure. Piezoelectric ceramics are perhaps the most popular piezoelectric materials for sensing purpose. In particular, sensors made of piezoelectric ceramic patches have recently gained increasing popularities in the field of structural health monitoring. For example, recent research works by Ayres, *et al.* (1998), Park, *et al.* (2003), Giurgiutiu (2003) and Ihn and Chang (2004) on piezoelectric (ceramic patch) sensor has made it a quite promising technique for nondestructive evaluation (NDE) applications.

*Corresponding Author, E-mail: zyf@umd.edu

As of today, most piezoelectric sensors are made of piezoelectric ceramics such as lead-zirconate-titanate (PZT). However, limitations of the mechanical properties of PZT such as brittleness and cracking at large deformations could impede its use in certain applications. Additionally, prefabricated PZT wafers do not fit well on surfaces with complex geometry such as welded joints. To overcome these problems associated with conventional piezoelectric ceramics, polymer-based piezoelectric paints have been investigated by a few researchers as a potential substitute for piezoelectric ceramics in certain sensing applications (Hanner and Safari 1989, Egusa and Iwasawa 1993, 1996 & 1998, Wenger, *et al.* 1996, Hale and Tuck 1999, Badcock and Birt 2000, Sakamoto, *et al.* 2001a and 2001b, White, *et al.* 2004, Zhang 2006, Lahtinen, *et al.* 2007). Piezoelectric paint typically comprises of tiny piezoelectric particles randomly dispersed within a polymer matrix and therefore is classified as piezoelectric 0-3 composite.

Recently, piezoelectric paint that uniformly cures at ambient temperatures after spray painting has been studied by Zhang and Li (2006) as sensing material for ultrasonic NDE application. Spray painting represents an inexpensive way to apply this novel sensor technology over large surface areas of a host structure, especially for those with curved surfaces or complex geometries. To achieve the low viscosity suitable for spray painting, the volume fraction of piezoelectric ceramic powder in the paint should be controlled below 45% based on the writers' experience. The values of piezoelectric charge coefficient d_{33} for piezoelectric paint formulations with 30 to 45% volume fraction of PZT generally fall between 5 and 20 pC/N, depending on the fabrication method employed (i.e. tape casting or hot press methods) and poling conditions (Zhang 2008).

This paper reviews and investigates the sensing capability of piezoelectric paint in the ultrasonic range up to several hundreds kilo Hertz. The underlying sensing principle of piezoelectric paint is first reviewed in the paper. The experimental results from preliminary ultrasonic tests including pitch-catch and pencil break tests are presented, which validated the wide-band ultrasonic sensing capability of piezoelectric paint. A finite element model that simulates the ultrasonic test of piezoelectric paint sensor was calibrated with experimental data and a parametric study using this finite element model provides useful information for transducer design. From this study, it appears that piezoelectric paint sensor provides a promising wide-band low-profile surface-mount or embeddable ultrasonic transducer for *in situ* structural health monitoring. It is also noted the results presented here are from a preliminary study of piezoelectric paint and a more comprehensive experimental program needs to be carried out to fully characterize the ultrasonic sensing characteristics of piezoelectric paint such as dielectric loss, mechanical and electrical quality factors, and electromechanical coupling factor in radial mode.

2. Piezoelectric 0-3 composite for ultrasonic sensing application

Piezoelectric composite materials consisting of ferroelectric ceramics and polymer (e.g. Safari 1994, Chilton 1995, Akdogan, *et al.* 2005) have received considerable interest as sensing elements because of their favorable material properties not easily attainable in a single-phase material. Through judicious selection of the polymer matrix, the composite properties of the piezoelectric paint can be tailored to meet the specific requirements of an application conditions. For example, piezoelectric paint might be more suitable for use in fiber-reinforced-polymer composite structures because of its improved acoustic impedance matching property compared to piezoelectric ceramics.

Piezoelectric composites can be classified according to the connectivity of piezoelectric ceramics and matrix phases (Newnham, *et al.* 1978). Piezoelectric paint typically comprises tiny piezoelectric

particles mixed within polymer matrix and therefore belongs to the “0-3” piezoelectric composite. The “0-3” means that the piezoelectrically-active ceramic particles are randomly dispersed in a 3-dimensionally connected polymer matrix. Conceivably, “0-3” piezoelectric composites can be more easily fabricated in complex shapes than other forms of composites. In general, the 0-3 composite family has been found to exhibit high hydrostatic piezoelectric voltage coefficients when compared to the properties of conventional single phase materials (Hanner, *et al.* 1989).

In the past two decades, the feasibility of using piezoelectric paint for ultrasonic signal sensing has been experimentally demonstrated by Egusa and Iwasawa (1996), Wenger, *et al.* (1996), Sakamoto, *et al.* (2001b), Marin-Franch, *et al.* (2004), and Kobayashi, *et al.* (2007). In particular, acoustic emission (AE) sensing with piezoelectric paint sensor is a promising new approach to fracture detection: low-cost piezoelectric paint sensor array can be attached to the neighborhood of hot spot areas in a structure and such close range AE monitoring can avoid the signal attenuation problem associated conventional AE sensors. Naturally, AE waveform based signal interpretation, which is very challenging for conventional AE technique due to external noise (such as vehicles crossing bridges) and travel path complexity (from AE source to sensor), could be realized in piezoelectric paint based AE method for fracture monitoring.

Egusa and Iwasawa (1993) prepared an epoxy resin-based piezoelectric paint with 53% volume percent PZT powder as filler. The 152- μm thick paint film was then cured in air at room temperature for at least three days or at 150 °C for 45 min. The piezoelectric sensitivity of the paint film as an acoustic emission sensor was evaluated in their study (Egusa and Iwasawa 1996). A nearly flat frequency response of the paint film to AE waves was observed in the frequency range above 0.3 MHz.

0-3 piezoelectric composites, consisting of a ferroelectric ceramic powder of calcium modified lead titanate (PTCa) dispersed in a polymer matrix, have been fabricated and their ferroelectric properties have been investigated by Wenger, *et al.* (1996). Two formulations of 0-3 composites, one with a copolymer of polyvinylidene trifluoroethylene (P(VDF-TrFE)) and the other with a thermosetting epoxy resin, was studied. The composite of the ceramic with the epoxy, PTCa/epoxy in a 60/40 volume per cent, was prepared by gradually adding the ceramic powder to the resin while stirring continuously to ensure an even mixture (Wenger, *et al.* 1996). The ceramic/copolymer composite PTCa-P (VDFTrFE) with a 65/35 volume fraction was prepared by a hot-rolling technique. The d_{33} coefficients for the composites of PTCa/P (VDF-TrFE) and PTCa/Epoxy are 33 pC/N and 26 pC/N respectively. Surface mounted AE sensors were fabricated using the composite films thus obtained and their frequency response was evaluated using a face-to-face technique over the frequency range of 300 kHz to 50 MHz. Embedded transducers, constructed from the piezoelectric composite films were used to detect plate waves within a laminate glass/epoxy plate measuring 304.8-mm \times 304.8-mm \times 1.9-mm. It was found in their study (Wenger, *et al.* 1996) that in the case of the embedded transducers, the PTCa/Epoxy films seem to be the better choice of transducer material, producing signals comparable in amplitude to those of an embedded PTCa/P(VDF-TrFE) film but more clearly defined.

Sakamoto, *et al.* (2001a) studied a flexible piezoelectric composite with 0-3 connectivity, made from PZT powder and castor oil based polyurethane (PU), which was doped with a small amount of fine-grained carbon powder to facilitate poling at relatively low electric field and in shorter time. The carbon particles located between the PZT particles help to create a continuous electric flux path. The PZT powder was mixed with carbon by a vibrator for 30 min prior to introducing this mixture in the polyurethane matrix. The composite was placed between two-paraffin paper and pressed at room temperature. The applied pressure was about 20 MPa and it was possible to obtain samples in the thickness range of 250 μm to 350 μm . After poling, the d_{33} coefficient was measured and it was observed that the highest value of d_{33} coefficient (around 12 pC/N) was achieved with PZT/C/PU

samples with 59/1/40 vol.% composition. The PZT/C/PU composite has shown the ability to detect both extensional and flexural modes of simulated acoustic emission at a distance of up to 8.0 m from the source (Sakamoto, *et al.* 2001b).

Badcock and Birt (2000) have examined the use of piezoelectric 0-3 composite as embedded Lamb wave sensors for damage detection in carbon fiber reinforced composite plates (E-glass/913 and T800/924 aerospace composites). The 0-3 composite consists of PZT-5H powder dispersed in an epoxy matrix. Cured PZT/epoxy materials with a PZT volume fraction of 60% was immersed in an oil bath for poling at a predefined temperature in the range of 50 °C to 120 °C. It was found that the greatest poling efficiency is achieved at 60 °C (most samples were poled at a field of 19 kV/mm for five minutes), with sensitivities of around 17 pC/N for the piezoelectric charge constant d_{33} . Comparative study of three different transducers – a conventional PZT ultrasonic transducer, a 500- μm thick PVDF element, and a 600- μm thick piezoelectric 0-3 composite film, were carried out to receive the Lamb wave signal at a fixed distance from the transmitting transducer. It was found the piezoelectric 0-3 composites were twice as sensitive when compared to PVDF films.

In this study, PZT-5A powder was chosen as active piezoelectric ingredient for the paint since PZT-5A has a high stability with time and temperature that means it is useful under a wide variety of environments. Additives such as dispersing agents and defoamers were also added to the paint mixture during the paint grinding and mixing process. The epoxy resin used in this study is a liquid resin comprised mainly of Diglycidyl Ether of Bisphenol A (DGEBA). The wet paint was first deposited to a flat PVC plate. After five days of curing at room temperature, the paint sample was then peeled off from the PVC plate. The volume fraction of PZT powder in the cured paint is about 42%. As shown in Fig. 1, the cured paint sample is fairly flexible. Silver paint was applied onto the both sides of the piezoelectric paint film sample for electrodes before oil bath poling. Poling of ferroelectric materials to induce piezoelectricity is an important step in the manufacturing of piezoelectricity-based sensors. The poling process switches the polar axis of crystallites to the symmetry-allowed directions nearest to that of the externally applied electrical field. After the curing and electroding process had been completed, poling of the piezoelectric paint was carried out to activate its piezoelectric effect. In this study, poling of the paint film was carried out in oil bath under a field of 8 MV/m at 70 °C for one hour to activate its piezoelectric effect. The poled paint sensor has a d_{33} value of 11 pC/N which was measured using a d_{33} meter from KCF Technologies. The paint film thickness was about 0.6 mm as measured using a micrometer.



Fig. 1 Picture of flexible piezoelectric paint

3. Sensing principle of piezoelectric paint

This section describes the sensing mechanism of piezoelectric paint, which generates electric voltage when subjected to mechanical strain in its film plane.

3.1. Electromechanical relation of piezoelectric paint

Like all other piezoelectric materials, piezoelectric paint can produce electric voltage signals proportional to the applied mechanical deformation in its film plane. The derivation below formulates the voltage-strain relationship of piezoelectric paint. In general, the relationship between the electrical and mechanical properties of piezoelectric materials can be expressed by the following constitutive equations (IEEE Standard 1987),

$$D_i = e_{ij}^\sigma E_j + d_{im}^d \sigma_m \tag{1a}$$

$$\varepsilon_k = d_{jk}^c E_j + s_{km}^E \sigma_m \tag{1b}$$

where $i, j = 1, 2, 3$ and $k, m = 1, 2, \dots, 6$. Here, D, E, σ , and e are the dielectric displacement, electric field, stress, and strain, respectively; e_{ij}^σ, d_{jk}^c (or d_{jk}^d), and s_{km}^E are the dielectric permittivity (Farad/m), the piezoelectric coefficients (Coulomb/N or m/Volt), and the elastic compliance (m^2/N); the piezoelectric coefficient d_{jk}^c defines the strain per unit electric field at constant stress and d_{jk}^d defines electric displacement per unit stress at constant electric field. The superscripts c and d are used to distinguish between the converse and direct piezoelectric effects, though in practice, these coefficients are numerically equal (Sirohi and Chopra 2000). The superscripts σ and E indicate that the quantity is measured at constant stress and constant electric field, respectively.

Eq. (1-a) is the sensor equation and Eq. (1-b) is the actuator equation. Sensor applications are based on the direct piezoelectric effect. When a stress is applied to the piezoelectric paint film in a transverse direction (perpendicular to the polarization direction 3), a voltage is generated which tries to return the piece of piezoelectric paint to its original length and width. In the case of a sensor, where the applied external electric field is zero, Eq. (1-a) becomes.

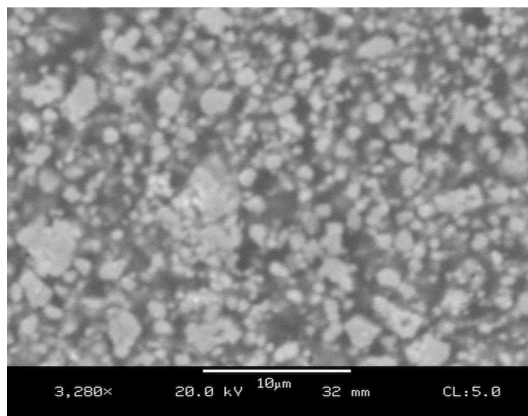


Fig. 2 Scanning electron microscope picture of piezoelectric paint (42% PZT volume fraction)

$$\begin{Bmatrix} D_1 \\ D_2 \\ D_3 \end{Bmatrix} = \begin{bmatrix} 0 & 0 & 0 & 0 & d_{15} & 0 \\ 0 & 0 & 0 & d_{24} & 0 & 0 \\ d_{31} & d_{32} & d_{33} & 0 & 0 & 0 \end{bmatrix} \{\sigma_1 \ \sigma_2 \ \sigma_3 \ \sigma_4 \ \sigma_5 \ \sigma_6\}^T \quad (2)$$

where $\{\sigma_1 \ \sigma_2 \ \sigma_3 \ \sigma_4 \ \sigma_5 \ \sigma_6\}^T = \{\sigma_{11} \ \sigma_{22} \ \sigma_{33} \ \sigma_{23} \ \sigma_{31} \ \sigma_{12}\}^T$; therefore, σ_4 , σ_5 and σ_6 are shear stress. A piezoelectric paint sensor can be modeled as a thick film capacitor mounted on the surface of host structures. The polarization direction which is usually along the thickness is denoted as the 3-axis; the 1-axis and 2-axis are in the film plane of the piezoelectric paint.

3.2. Effect of coupling between piezoelectric sensor and host structure on strain sensing

Without loss of generality, in this section we assume that piezoelectric paint sensor is only subjected to unidirectional strain in its film plane. The dielectric displacement D_3 is related to the generated electric charge by the following relationship,

$$q = \iint D_3 dA_3 \quad (3)$$

where dA_3 is the differential electrode area in the 1-2 plane of the piezoelectric paint.

From Eqs. (1) to (3), the electric charge generated by the sensor is

$$q = d_{31} Y_C b_c \int_{l_c} \varepsilon_1 dl \quad (4)$$

where Y_C is the Young's modulus of the piezoelectric paint, l_c and b_c are length and width of the piezoelectric paint sensor, respectively.

When used as actuators/sensors for smart systems, piezoelectric patches (e.g. PZT wafer or PVDF film) are usually bonded to the surface of the host structure. Due to material mismatch between the piezoelectric patch and host medium, and the electro-mechanical property of piezoelectric materials, it is very challenging to analytically express the interaction behavior between the host structure and surface-mounted or embedded piezoelectric actuator/sensor. Crawley and de Luis (1987) presented a comprehensive analytical and experimental work of using piezoelectric ceramic patch as distributed actuators of intelligent structures. They carried out an one-dimensional elastic analysis of dual surface mounted piezoelectric ceramic patches which were used to excite the bending and extension modes in a beam-like structure by assuming a linear Bernoulli-Euler strain distribution across the actuator (i.e., the piezoelectric patch) thickness, pure one-dimensional shear in bonding layer and linear strain distribution within the structure. Based on a simplified model for the strain transfer from the actuator to the structure by an adhesive bonding layer, they successfully predicted the bending and extension modes in the host structure as well as the shear lag effect in the bonding layer. Eqs. (3) and (4) above were derived in a similar fashion based on a simplified bonding layer model.

Furthermore, using this simplified bonding layer model, it can be shown that piezoelectric paints can be used as strain sensor or strain rate sensor due to the electro-mechanical coupling property of piezoelectric materials. Lee and O'Sullivan (1991) investigated piezoelectric strain rate gages used for measuring dynamic friction force variation and in strain rate control of flexible structure. Based on linear piezoelectric theory and Kirchhoff hypothesis (i.e., any line perpendicular to the beam or plate

mid-plane remains perpendicular to the mid-plane after deformation), they proposed that the closed-circuit current signal generated in a surface-bonded piezoelectric patch is proportional to the strain rate of the host structure. Since current is the rate of change of electric charge, measuring the electrical current generated by the piezoelectric patch is equivalent to measuring strain rate. By using a simple current amplifier the piezoelectric sensor measures the strain rate directly and is more accurate in comparison with the differentiated signal from conventional foil strain gage measurements.

In summary, when a current amplifier is used as the signal conditioning circuit, the voltage output of the sensor can be expressed as

$$V_{out}(t) = -R_f \dot{q} = -R_f d_{31} Y_C b_C \int_{l_c} \dot{\epsilon}_1 dl \quad (5)$$

the output voltage is proportional to the integral of time derivative of the in-plane strain in 1-direction.

Sirohi and Chopra (2000) studied the behavior of PZT and PVDF strain sensor over a frequency range of 5 to 500 Hz. In their work, a typical piezoelectric patch sensor is considered as a parallel plate capacitor, which stores the electric charge generated by the piezoelectric sensor when mechanical deformation is applied. They analytically derived and experimentally verified that if only one-dimensional in-plane deformation is considered, the voltage generated across the electrodes of the capacitor can be related to the average in-plane strain by a sensor sensitivity parameter and the sensor capacitance (see Eq. (4) and considering the relation between charge and voltage, $q = V_c C_p$). In order to account for the coupling effect between the piezoelectric patch sensor and host structure, several correction factors have been introduced to achieve accurate measurement. A charge amplifier was used in their investigation as the signal conditioning circuit to measure the charge generated by the sensor, which is proportional to the mechanical strain at the host structure location of the sensor. A beam bending test was performed in their work to show that piezoelectric strain sensors are more sensitive and have low noise-to-signal ratio when compared with metal foil strain gages.

In summary, if a charge amplifier is connected to the sensor electrode, then the output voltage is

$$V_{out}(t) = \frac{q}{C_f} = \frac{d_{31} Y_C b_C}{C_f} \int_{l_c} \epsilon_1 dl \quad (6)$$

Therefore, the sensor output voltage is proportional to the integral of the in-plane strain in 1-direction.

In addition to the one-dimensional beam model, plate and shell theory have also been used to model the behavior of surface bonded piezoelectric patches. Lee (1990) formulated the general governing equations of piezoelectric laminate used as distributed actuators/sensors. The effects of different boundary conditions were studied in their work. It is pointed out by Piefort (2001) that when the thickness of piezoelectric patch becomes comparable to that of the host structure, the use of shell model is necessary to account for in-plane deformations.

In recent years, the potential of using piezoelectric patches as low profile ultrasonic transducer for in-situ structure health monitoring has attracted great attention from many researchers (e.g. Lin and Giurgiutiu 2006, Wang and Huang 2006). Different from dynamic strain/strain rate measurement applications (i.e. low frequency application), in which the vibration wavelength is much larger than the size of piezoelectric sensor, ultrasonic waves propagating in the host structure often has a wavelength comparable to or less than typical sensor size. Wang and Huang (2006) studied the behavior of piezoelectric sensors bonded to an elastic half space under high frequency loading. A one-dimensional sensor model considering the effect of sensor stiffness has been developed in their study. The analytical solution given by Wang and

Huang (2006) shows that flexible and smaller sensor size are desired to enable reliable high frequency sensing by piezoelectric sensor.

4. Experimental study on ultrasonic sensing capability of piezoelectric paint

4.1. Basics of guided wave theory

The elastic wave propagation theory has been an important subject in nondestructive evaluation (NDE). Elastic waves in solid media are commonly divided into two groups: body waves and guided waves. As typical guided waves, Lamb waves represent elastic wave propagating in a thin plate with free boundaries. There are two groups of Lamb waves with different modes – symmetrical and anti-symmetrical. In a plate with a thickness of $2d$, a finite number of symmetrical and anti-symmetrical modes of Lamb wave may co-exist at a given frequency ω . Each can travel independently through the plate structure at different phase velocity, satisfying the governing equations and boundary conditions.

The major difference between body wave propagation and guided wave propagation exists in the fact that a boundary is required for guided wave propagation. When a group of guided waves travel through a thin plate like structure, a variety of waves will reflect along the structure boundaries and different modes convert inside the structure and superimpose with areas of defects that finally leads to the nicely behaved guided wave packets that can travel in the structure (Rose 2002).

Phase velocity is one of the important characteristics of Lamb wave. Once it is known, the particle motion and displacements of any point in the plate like structure can be determined. To find the phase velocities of symmetrical and anti-symmetrical modes, Rayleigh-Lamb equations (Viktorov 1967) are solved numerically.

$$\frac{\tan(\sqrt{1-\zeta^2}d)}{\tan(\sqrt{\xi^2-\zeta^2}\bar{d})} = -\frac{4\zeta^2\sqrt{1-\zeta^2}\sqrt{\xi^2-\zeta^2}}{(2\zeta^2-1)^2}, \quad \text{for symmetrical modes} \quad (7)$$

$$\frac{\tan(\sqrt{1-\zeta^2}\bar{d})}{\tan(\sqrt{\xi^2-\zeta^2}d)} = -\frac{(2\zeta^2-1)^2}{4\zeta^2\sqrt{1-\zeta^2}\sqrt{\xi^2-\zeta^2}}, \quad \text{for antisymmetrical modes} \quad (8)$$

where $\zeta^2 = c_t^2/c^2$, $\xi^2 = c_l^2/c_t^2$ and non-dimensional frequency thickness product $\bar{d} = \frac{\omega}{c_t}d$, c_l , c_t and c are the phase velocity of longitudinal, transverse and Lamb wave respectively. A detailed discussion of the solution strategy for the above equations can be found in the reference by Rose (1999).

4.2. Impedance measurement of piezoelectric paint sensor

The impedance curves of both piezoelectric paint sensor and PZT sensor were measured using an HP 4192A impedance analyzer by sweeping over an ultrasonic frequency range from 10 kHz to 1MHz. For a piezoelectric material, the elastic field and electric field in the material is coupled through the piezoelectric effect, which means mechanical stress wave can be generated by applying an electrical excitation to the material or vice versa. Resonance frequencies of a material can be observed in impedance measurement which depends on the specific combination of specimen geometry and boundary conditions.

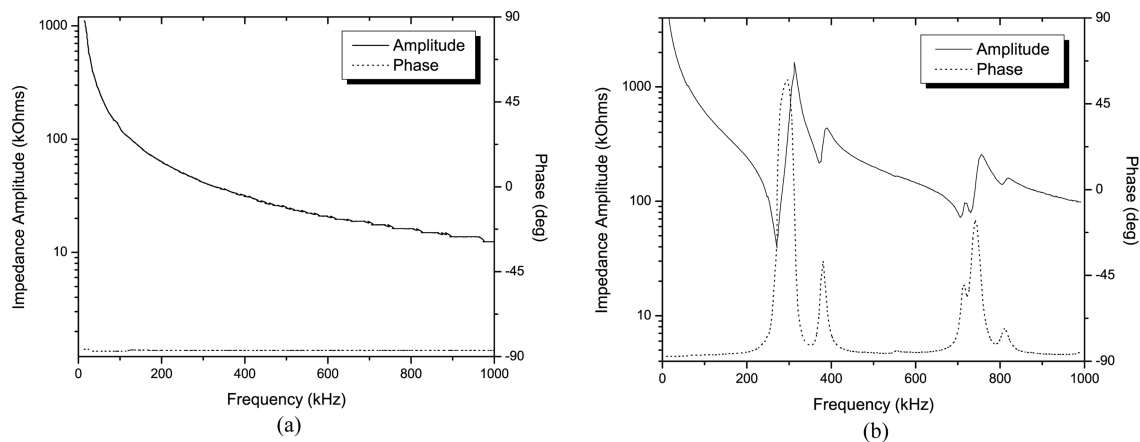


Fig. 3 Impedance measurement of (a) piezoelectric paint with 42% volume fraction of PZT powder (b) PZT patch with a 0.2-mm thickness

The resonance frequencies for piezoelectric specimens with free boundary can be found from measured impedance curve of the material. Figs. 3(a) and 3(b) show the impedance magnitude and phase angle of the piezoelectric paint sensor with a size of $7\text{ mm} \times 7\text{ mm} \times 0.6\text{ mm}$ and PZT sensor with a size of $7\text{ mm} \times 7\text{ mm} \times 0.2\text{ mm}$. It is seen that several resonance peaks occur over the specified ultrasonic frequency range for the PZT ceramic patch, while the piezoelectric paint sensor shows a relatively smooth impedance curve with no resonance peak over this frequency range. The fact that the resonance frequency of piezoelectric paint is outside the frequency range of importance to ultrasonic based NDE suggests that piezoelectric paint has the potential to make wide-band ultrasonic transducer. This feature of piezoelectric paint makes it a favorite candidate material for next-generation wide-band low-profile acoustic emission sensor that enables waveform based acoustic emission signal interpretation.

4.3. Ultrasonic sensing test of piezoelectric paint sensor

This section describes the preliminary results from a series of ultrasonic tests conducted to investigate the ultrasonic sensing capability of piezoelectric paint sensor. Two types of ultrasonic tests were conducted – ultrasonic pitch-catch test which involves measuring guided waves in thin plate with piezoelectric paint sensor and pencil break test to simulate acoustic emission source.

4.3.1. Pitch-catch test of piezoelectric paint sensor

A pitch-catch ultrasonic test was conducted to examine the sensing capability of piezoelectric paint sensor over ultrasonic frequency range. The piezoelectric paint sensors were deposited to a $609.6\text{ mm} \times 609.6\text{ mm} \times 1.59\text{ mm}$ aluminum plate. A layer of conductive silver paint is applied on top of the piezoelectric paint having a size of $7\text{ mm} \times 7\text{ mm}$. After curing and electroding had been completed, poling of the piezoelectric paint was carried out to activate its piezoelectric effect. A $7\text{ mm} \times 7\text{ mm} \times 0.2\text{ mm}$ piezoelectric ceramic (APC850 manufactured by American Piezo Ltd.) patch was also bonded along the center line of the piezoelectric paint sensors as the actuator to excite lamb waves in the aluminum plate.

Fig. 4 shows the ultrasonic test setup. A five-cycle windowed tone-burst excitation signal was generated by an Agilent 33220A function generator at various frequencies. Generally, guided waves propagating through metal structure surface are highly dispersive and tend to decay very fast with the increase of

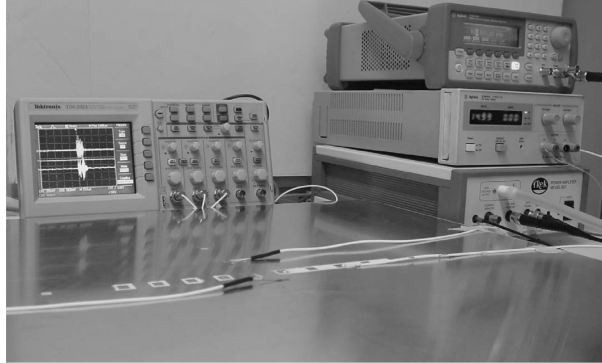


Fig. 4 View of the ultrasonic test setup

the propagation distance. In order to receive a clear, high quality signal, a wideband power amplifier (Trek model 603) is used to provide high voltage excitation signal to the PZT wafer so that the excited guided waves could cover a larger area with high signal-to-noise ratio. Piezoelectric paint sensors were used to measure the guided wave propagation at corresponding sensor locations. An AD745 high frequency wideband operational amplifier circuit with 40 dB gain was connected with the piezoelectric paint sensor as a charge amplifier and then the amplified signal was recorded with a Tektronix TDS 2024 oscilloscope connected to a computer via a GPIB adapter.

In this test, the PZT wafer was excited by 10 V peak-to-peak voltage signal to eject lamb wave into the aluminum sheet. Ultrasonic lamb waves were received by a piezoelectric paint sensor which is 102 mm away from excitation. Before raw sensor data can be interpreted to determine structural health condition, signal processing is necessary to ease the interpretation process. This is especially true for piezoelectric paint sensor because of its low sensitivity and hence low signal-to-noise ratio compared to PZT sensor. In the present research, discrete wavelet transform (DWT) technique was used to filter the signal captured by piezoelectric paint sensor.

Wavelet transform is similar to Fourier analysis, but instead of breaking up a signal into sinusoids at different frequencies wavelet transform breaks up signal into shifted and scaled complex “mother wavelets”. Wavelet transform is a linear transform, and the process can be applied in continuous or discrete form. In practical, DWT is more preferable because of two reasons: (i) most of the mother wavelets do not have close-form solution; (ii) to reduce computational intensity. Mathematically, DWT can be expressed as

$$W(j, k) = \frac{1}{\sqrt{a^j}} \int_{-\infty}^{\infty} x(t)g^*(a^{-j}x - kb)dt \quad (9)$$

where a is the scale factor, b is the time shift, $x(t)$ is original signal, $g^*(t)$ is the complex conjugate of the basic wavelet $g(t)$ and $W(a, b)$ is the wavelet coefficient. k, j are integers.

Scales and positions are usually chosen based on powers of two which are so-called “dyadic” scales and positions (Misiti, *et al.* 2000). Then, the DWT is

$$W(j, k) = \frac{1}{\sqrt{2^j}} \int_{-\infty}^{\infty} x(t)g^*(2^{-j}x - kb)dt \quad (10)$$

A fully recovery of the original signal, or the inverse of the above procedure, is performed as follows

$$x(t) = \sum_{j,k} W(j, k)g_{j,k}(t) \tag{11}$$

where

$$g_{j,k}(t) = \frac{1}{\sqrt{2^j}}g(2^j t - k) \tag{12}$$

The application of DWT to waveform signals results in the decomposition of original signal into a variety of wavelet scales. Each scale represents a certain frequency band and the sum of all scales reconstructs the original signal. By retaining selected wavelet scales of the original signal, wavelet decomposition works as a band-pass filter.

Matlab® was used to perform the signal de-noising since this software provides a convenient wavelet toolbox. The Daubechies wavelet db6 at level 5 was used for decomposition because the shape of this wavelet is close to the driving burst signal, thus making the process accurate and efficient (Kessler 2002).

Fig. 5 plots the DWT-filtered paint sensor signals at 100 kHz, 200 kHz, 300 kHz and 400 kHz excitation frequencies. The filtered signals clearly show the propagation of Lamb waves over time. From this figure, two waveforms - A0 and S0 modes can be easily identified. It is seen that under the same excitation frequency the S0 wave propagates faster than the A0 wave. The S0 wave travels in the aluminum sheet at a group speed nearly independent of frequency which approximately equals to 5.3 km/s. At 300 kHz excitation, the S0 wave achieves its strongest amplitude while the A0 wave becomes

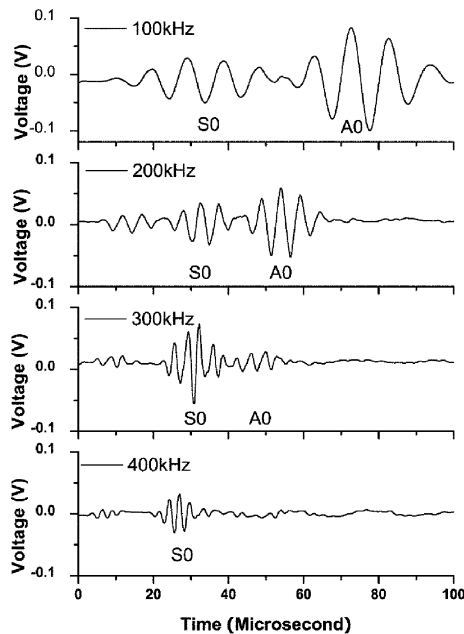


Fig. 5 Filtered pitch-catch ultrasonic signal received by piezoelectric paint sensor (with a 40 dB amplifier) under 100 kHz, 200 kHz, 300 kHz and 400 kHz excitation (arranged from top to bottom)

barely detectable by paint sensor. This consists with the theoretical calculation performed by Giurgiutiu (2005) that 300 kHz was identified as the preferential excitation frequency for S0 mode wave in the 1.59-mm thick aluminum sheet. With the increasing of driving frequency from 100 kHz to 400 kHz, the group speed of A0 wave increases and the amplitude drops.

4.3.2. Acoustic emission test of piezoelectric paint sensor

Acoustic emission (AE) consists of a propagating elastic wave generated by a sudden release of energy within a material. In recent years, AE has been shown to provide real-time information on the progression of damage within metallic structures. The elastic wave generated by structural damage propagates through the solid to the surface where it can be detected by surface mounted sensors. The sensor captured AE waveforms contain information about the damage source, like location, size and type etc, it is possible to extract such information by analysis those waveforms. Different from ultrasonic active sensing which intentionally excites elastic waves in a solid, AE sensors passively listen for acoustic signals generated by crack initiation and progression. Acoustic emission (AE) has been proved as a useful NDE method for the investigation of local damage in structural members.

In order to verify the capability of piezoelectric paint sensor as acoustic emission sensor, pencil beak test was performed on the same aluminum plate as in the previously described ultrasonic test. Pencil break source (also called Hsu-Neilsen source) is a common approach to simulate acoustic emission due to its simplicity and reproducibility. In this study, a pencil lead with a 0.5-mm diameter was broken by pressing against the aluminum plate to simulate acoustic emission from progression of a micro-crack. The same data acquisition equipment as in the ultrasonic test was used here. For comparison purpose, a 7 mm × 7 mm × 0.2 mm PZT sensor has been placed right next to the piezoelectric paint sensor on the aluminum plate to capture the AE signal. A charge amplifier with gain of 26 dB was used in the piezoelectric paint sensor. The pencil lead was fractured at the same distance of 127 mm (~5 in) away from both the PZT and paint sensor. Fig. 6 plots the filtered AE signals collected at a sampling rate of 2.5 MHz. The db6 level 5 wavelet was used to filter the measured AE signals. The both PZT sensor (without amplifier) and piezoelectric paint sensor (with amplifier) gave a peak-to-peak response around 50 mV. The two signals agree with each other very well. This preliminary test verifies the potential application of piezoelectric paint sensor in real-time monitoring of the crack initiation and propagation in metal structures.

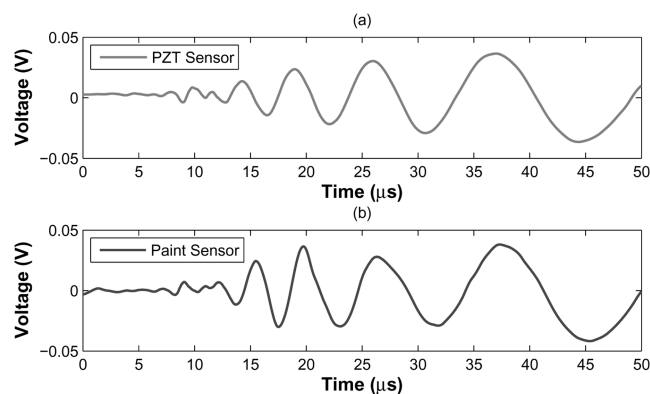


Fig. 6 AE signal received by piezoelectric sensors in pencil break test: (a) PZT sensor (without preamplifier); (b) Piezoelectric paint sensor (with a 26 dB amplifier)

5. Finite element simulation

Though many early works (e.g. Viktorov 1967, Rose 1999) have developed analytical or semi-analytical solutions to the problem of guided wave propagation in elastic solid media, those solutions are only available to rather simple geometries like elastic half-space or infinitely large plate. However, structural geometries in practical applications are of finite dimensions and usually contain complex details such as curved surfaces and connections. Recently, with increasing computer power and availability of powerful commercial finite element simulation software, the use of finite element (FE) to study ultrasound generation and propagation in elastic body has been quickly growing in popularity. It has been shown in many researchers' work that FE can effectively simulate complex elastic guided wave behavior with various source configurations, specimen geometries and material properties (e.g. Hamstad, *et al.* 1996, Kessler 2002, Lee and Staszewski 2003).

In this section, guided wave propagation in an aluminum plate is numerically simulated by using a popular finite element package - ABAQUS/Explicit. The reason for choosing ABAQUS/Explicit code over ABAQUS/Standard is that ABAQUS/Explicit uses an explicit time integration method which is well suited for solving high speed, transient dynamic problems. In this study, the aluminum plate is assumed to be infinitely long in its width direction such that a 2-dimensional model representing the plate specimen for both the ultrasonic test and AE test above can be established using plane strain condition. Since the plate is symmetrical and excitations for both tests were applied at the center of the plate, only half of the plate, which measures 1.59 mm in thickness and 400 mm in length, was modeled for reduced computational effort. The maximum element length in the wave propagation path was chosen to be substantially smaller than one-eighth of the smallest wave length of interest to ensure the convergence of the simulation results (see, e.g. Nieuwenhuis, *et al.* 2005). ABAQUS/Explicit uses the central-difference operator for transient dynamic analysis. Because the central-difference method is only conditionally stable, the maximum time increment in this simulation study was chosen to be less than 1/20 of the shortest wave period to ensure numerical stability.

From Eq. (6), when a charge amplifier is used, the output voltage of piezoelectric paint sensor is proportional to the integral of the in-plane strain at the location of the sensor. Therefore, instead of building a fully coupled electro-mechanical piezoelectric sensor model to simulate wave detection, the detected voltage can be approximately predicted as the sum of the in-plane strain of the plate elements at which the paint sensor is located. The material properties of the aluminum plated used in this study are as follows: Young's modulus $E = 70$ GPa; Poisson's ratio $\nu = 0.33$ and density; $\rho = 2700$ kg/m³.

5.1. Numerical simulation of guided wave propagation

A surface mounted PZT excitation source was modeled as a pair of time-dependent concentrated forces applied at the end points of the PZT patch to excite ultrasonic wave propagation in the plate. The excited tone-burst signal can be expressed by

$$F(t) = \begin{cases} F_0 \sin(\omega t) \cdot \left(\sin\left(\frac{\omega t}{10}\right)\right)^2 & t < \frac{10\pi}{\omega} \\ 0 & \text{otherwise} \end{cases} \quad (13)$$

where ω is the center angular frequency of the windowed tone-burst excitation signal.

After several convergence tests, a total of 3200 four-node plain strain elements were used in the finite

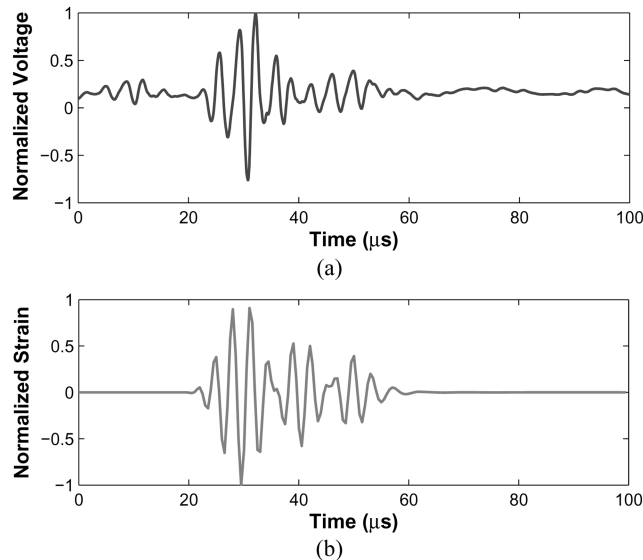


Fig. 7 Pitch-catch ultrasonic signal received by piezoelectric paint sensor in pitch-catch test at 300 kHz excitation: (a) Experimental data; (b) FE simulation data

element model to achieve the desired accuracy. Fig. 7 shows simulation results at an excitation frequency of 300 kHz along with corresponding experimental data. The simulated sensor response shows very good agreement with the measured data. It is thus concluded that the summation of the in-plane strain times a proportional constant provides a good approximation to the real voltage signal.

5.2. Numerical simulation of acoustic emission test

The interpretation of AE signal to derive any meaningful information about structural condition is rather challenging because of the complex and transient nature associated with the AE phenomenon (see, e.g. Grosse and Ohtsu 2008). A variety of factors such as AE source mechanism, structural geometry, material property, characteristics of sensor and data acquisition system, and operating environment all have certain impact on the information carried by the measured AE signals. Therefore, the ability of accurately modeling the AE phenomenon is desired to improve the understanding of the AE mechanism.

Pencil lead break has been widely used to generate AE source in many experimental study of AE wave propagation in engineering structures. The simulated acoustic emission source can be analytically modeled as a sudden release of the applied stress. In FE simulation of pencil break test, the key parameters of this time dependent stress including stress amplitude, source size and rise time have been studied by a number of researchers including Breckenridge, *et al.* (1990) and Hamstad, *et al.* (1996). In this study, an analytical model that follows the previous work by Hamstad, *et al.* (1996) was used to model the AE source as an out-of-plane ramp load with the following parameters: peak amplitude on the order of 1 N, rise time less than 1 μ s, and the circular source diameter less than 3 mm. The simulated AE source was applied at 50.8 mm away from paint sensor center point.

Fig. 8 plots the simulated AE test signal as well as experimental data from piezoelectric paint sensor. Although close agreement between the simulated response and the sensor measured voltage can be observed, some level of discrepancy does exist between these two waveforms. When Lamb wave

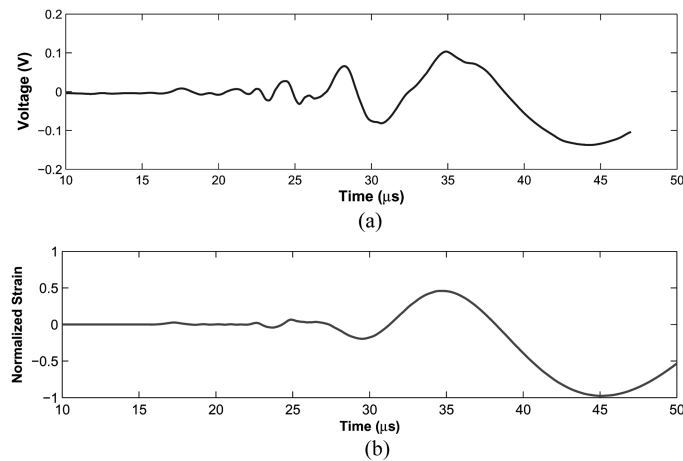


Fig. 8 AE signal received by piezoelectric paint sensor located at 50.8 mm away from pencil break: (a) filtered experimental data (with a 26 dB amplifier); (b) FE simulation data

generated by a lead break source propagates through a plate like structure, its velocity and amplitude are dependent on the source frequency content and plate geometry. Because of this dispersion characteristic of lamb wave, it is believed that the differences mainly come from two sources: (i) idealization of lead break source as a vertical ramp load; (ii) inconsistency between the geometry of the simulation model and test specimen due to the manufacture tolerance of the aluminum plate.

6. Conclusions

This paper examines the feasibility of piezoelectric paint with low volume fraction of piezoelectric ceramic particles in ultrasonic sensing. With proper formulation and fabrication method, piezoelectric paint with a viscosity suitable for spray painting can be made to have a piezoelectric activity level comparable to that of ferroelectric polymer. Piezoelectric paint has several advantages for in situ structural health monitoring application including its adjustable mechanical properties and conformability to surface with complex geometry such as welds in steel structural joints. The bonding effect between the piezoelectric paint sensor and host structure is considered in this study.

Experiment was carried out to investigate the ultrasonic sensing characteristics of piezoelectric paint. Impedance of piezoelectric paint was measured over a frequency range up to 1 MHz and no resonance peak was observed. This demonstrates the wideband nature of piezoelectric paint sensor over this important ultrasonic frequency range commonly used in acoustic emission or guided wave sensing. Pitch catch and pencil break tests were performed to validate the ultrasonic sensing capability of piezoelectric paint sensor.

Finite element simulation was also performed to provide a fundamental understanding of ultrasonic wave sensing mechanism of piezoelectric paint sensor as well as provide a tool for transducer design. The finite element model was validated using the measured data from ultrasonic test of piezoelectric paint sensor. Based on the results of this experimental and finite element simulation study, it can be concluded that piezoelectric paint sensor has a great potential to be used as wide-band low-profile surface mount or embedded ultrasonic sensor for real-time monitoring of crack initiation and propagation in

metallic or fiber-reinforced-polymer composite structure. However, it should also be noted that the results presented here only represent an exploratory work in this field and further work needs to be done to implement the piezoelectric paint sensor in real-world structures.

Acknowledgments

The work described in this paper was partially supported through a grant from the National Science Foundation under Award No. CMS-0442076 and CMMI-0726820 (program director: Dr. S.C. Liu). The authors are also grateful to the Pennsylvania Infrastructure Technology Alliance and Lehigh University for providing additional financial support for this research project. Partial financial support received by the second author from the University of Maryland to continue this research is also acknowledged. However, the opinions and conclusions expressed in this paper are solely those of the writers and do not necessarily reflect the views of the sponsors.

References

- Akdogan, E. K., Allahverdi, M. and Safari, A. (2005). "Piezoelectric composites for sensor and actuator applications," *IEEE Transactions on Ultrasonics, Ferroelectrics, and Frequency Control*, **52**(5), 746-775.
- Ayres, J. W., Lalande, F., Chaudhry, Z. and Rogers, C. A. (1998), "Qualitative impedance based health monitoring of civil infrastructures", *Smart Mater. Struct.*, **7**(5), 599-605.
- Badcock, R. A. and Birt, E. A. (2000), "The use of 0-3 piezocomposite embedded Lamb wave sensors for detection of damage in advanced fiber composites", *Smart Mater. Struct.*, **9**, 291-297.
- Breckenridge, F. R., Proctor, T. M., Hsu, N. N., Frick, S. E. and Eitzen, D. G., (1990), "Transient source for acoustic emission work", *Progress in Acoustic Emission V*, eds. Yamaguchi, K. et al, Japanese Society for NDI, Tokyo, 20-37.
- Chilton, J. A. (1995), "Electroactive composites", *Special Polymers for Electronics & Optoelectronics*, Edited by J.A. Chilton, M.T. Goosey, Chapman & Hall, London, 1995.
- Crawley, E. F. and de Luis, J. (1987), "Use of piezoelectric actuators as elements of intelligent structures", *AIAA J.*, **25**(10), 1373-1385.
- Damjanovic, D., Muralt, P. and Setter, N. (2001), "Ferroelectric sensors", *IEEE Sensors J.*, **1**(3), 191-206.
- Egusa, S. and Iwasawa, N. (1993), "Piezoelectric paints: preparation and application as built-in vibration sensors of structural materials", *J. Mater. Sci.*, **28**, 1667-1672.
- Egusa, S. and Iwasawa, N. (1996), "Application of piezoelectric paints to damage detection in structural materials", *J. Reinforced Plastics and Composites*, **15**, 806-817.
- Egusa, S. and Iwasawa, N. (1998), "Piezoelectric paints as one approach to smart structural materials with health-monitoring capabilities", *Smart Mater. Struct.*, **7**, 438-445.
- Gautschi, G. (2002), *Piezoelectric Sensorics*, Springer-Verlag, Berlin, Germany.
- Giurgiutiu, V. (2003), "Embedded ultrasonics NDE with piezoelectric wafer active sensors", *J. Instrumentation, Measurement, Metrology*, Lavoisier Pub., Paris, France, RS series 12M, **3**(3-4), 149-180.
- Giurgiutiu, V. (2005), "Tuned lamb wave excitation and detection with piezoelectric wafer active sensors for structural health monitoring", *J. Intell. Mater. Sys. Struct.*, **16**, 291-305.
- Grosse, C. U. and Ohtsu, M. (Eds.) (2008), *Acoustic Emission Testing: Basics for Research - Applications in Civil Engineering*. Springer Publisher, Heidelberg, Germany.
- Hale, J. M. and Tuck, J. (1999), "A novel thick-film strain transducer using piezoelectric paint", *Proc. Inst. Mech. Engrs., Part C*, **213**, 613-622.
- Hamstad, M. A., Gary, J. and O'Gallagher, A., (1996), "Far-field acoustic emission waves by three-dimensional finite element modeling of pencil-lead breaks on a thick plate", *J. Acoustic Emission*, **14**(2), 103-114.

- Hanner, K. A., Safari, A., Newnham, R. E. and Runt, J. (1989), "Thin film 0-3 polymer/piezoelectric ceramic composites: piezoelectric paints", *Ferroelectrics*, **100**, 255-260.
- IEEE Standard on Piezoelectricity. (1987), ANSI/IEEE, Standard 176.
- Ihn, J.-B. and Chang, F. K. (2004), "Detection and monitoring of hidden fatigue crack growth using a built-in piezoelectric sensor/actuator network: II. Validation using riveted joints and repair patches", *Smart Mater. Struct.* **13**, 621-630.
- Ikeda, T. 1990. *Fundamentals of Piezoelectricity*, Oxford University Press, Oxford, UK.
- Kessler, S. S. (2002), *Piezoelectric-Based In-Situ Damage Detection of Composite Materials for Structural Health Monitoring Systems*. PhD Thesis, Massachusetts Institute of Technology, Department of Aeronautics and Astronautics.
- Kobayashi, M., Jen, C-K, Moisan, J. F., Mrad, N. and Nguyen, S. B. (2007), "Integrated ultrasonic transducers made by the sol-gel spray technique for structural health monitoring", *Smart Mater. Struct.* **16**, 317-322.
- Lahtinen, R., Muukkonen, T., Koskinen, J., Hannula, S-P. and Heczko, O. (2007). "A piezopaint-based sensor for monitoring structure dynamics", *Smart Mater. Struct.*, **16**, 2571-2576
- Lee, C.-K., (1990), "Theory of laminated piezoelectric plates for design of distributed sensors/actuators. Part I: governing equations and reciprocal relationships", *J. Acoust. Soc. Am.*, **87**(3), 1144-1158.
- Lee, C.-K and O'Sullivan, T. C., (1991), "Piezoelectric strain rate gage", *J. Acoust. Soc. Am.*, **90**(2), 945-953.
- Lee, B. C. and Staszewski, W. J. (2003). "Modelling of Lamb waves for damage detection in metallic structures: Part I. Wave propagation", *Smart Mater. Struct.* **12**, 804-814.
- Lin, B. and Giurgiutiu, V., (2006), "Modeling and testing of PZT and PVDF piezoelectric wafer active sensors", *Smart Mater. Struct.* **15**, 1085-1093.
- Marin-Franch, P., Martin, T., Fernandez-Perez, O., Tunncliffe, D. L. and Das-Gupta, D. K. (2004), "Evaluation of PTCa/PEKK composites for acoustic emission detection", *IEEE Transactions on Dielectrics and Electrical Insulation*, **11**(1), 50-55.
- Misiti, M., Misiti, Y., Oppenheim, G. and Poggi, J. M., (2000), *Wavelet Toolbox for Use with MATLAB*, User's Guide, The MathWorks, Inc. MA, USA.
- Newnham, R. E., Skinner, D. P. and Cross, L. E. (1978), "Connectivity and piezoelectric-pyroelectric composites", *Mat. Res. Bull.* **13**, 525-536.
- Nieuwenhuis, J. H., et al. (2005), "Generation and detection of guided waves using PZT wafer transducers", *IEEE Transaction on Ultrasonics, Ferroelectrics, and Frequency Control*, **52**(11), 2103-2111.
- Niezrecki, C., Brei, D., Balakrishnan, S. and Moskalik, A. (2001), "Piezoelectric actuation: state of the art", *The Shock Vib. Digest*, **33**(4), 269-28.
- Piefort, V. (2001), "Finite element modeling of piezoelectric active structures", PhD Thesis, Universit'e Libre de Bruxelles.
- Park, G., Sohn, H., Farrar, C. R. and Inman, D. J. (2003), "Overview of piezoelectric impedance-based health monitoring and path forward", *The Shock Vib. Digest*, **35**(6), 451-463.
- Polla, D. L. and Francis, L. F. (1998), "Processing and characterization of piezoelectric materials and integration into microelectromechanical systems," *Annu. Rev. Mater. Sci.*, **28**, 563-97.
- Rose, J. L. (1999), *Ultrasonic waves in solid media*, Cambridge University Press, Cambridge.
- Rose, J. L. (2002), "A baseline and vision of ultrasonic guided wave inspection potential", *Trans. of ASME Journal of Pressure Vessel Technology*, **124**, 273-282.
- Safari, A. (1994), "Development of piezoelectric composites for transducer", *J. Phys. III France*, **4**, 1129-1149.
- Sakamoto, W. K., de Souza, E. and Das-Gupta, D. K. (2001a), "Electroactive properties of flexible piezoelectric composites", *Mater. Res.*, **4**(3), 201-204.
- Sakamoto, W. K., Marin-Franch, P., Tunncliffe, D. and Das-Gupta, D. K. (2001b), "Lead zirconate titanate / polyurethane (PZT/PU) composite for acoustic emission sensors", *IEEE Annual Conference on Electrical Insulation and Dielectric Phenomena*, **2001**, 20-23.
- Sirohi, J. and Chopra, I. (2000), "Fundamental understanding of piezoelectric strain sensors", *J. Intelligent Mater. Sys. Struct.*, **11**(4), 246-257.
- Viktorov, I. A. (1967), *Rayleigh and Lamb Waves – Physical Theory and Applications*, Plenum Press, New York.
- Wang, X. D. and Huang, G. L. (2006), "The coupled dynamic behavior of piezoelectric sensors bonded to elastic media", *J. Intell. Mater. Sys. Struct.*, **17**, 883-894.

- Wenger, M. P., Blanas, P., Shuford, R. J. and Das-Gupta, D. K. (1996), "Acoustic emission signal detection by ceramic/polymer composite piezoelectrets embedded in glass-epoxy laminates", *Poly. Eng. Sci.*, **36**(24), 2945-2954.
- White, J. R., de Poumeyrol, B., Hale, J. M. and Stephenson, R. (2004), "Piezoelectric paint: Ceramic-polymer composites for vibration sensors", *J. Mater. Sci.*, **39**(9), 3105-3114.
- Zhang, Y. (2006), "In-situ fatigue crack detection using piezoelectric paint sensor", *J. Intell. Mater. Sys. Struct.*, **17**(10), 843-852.
- Zhang, Y. and Li, X. (2006), "Piezoelectric paint sensor for fatigue crack monitoring in steel structures", Proc. US-Korea Workshop on Smart Structures Technology for Steel Structures, Seoul, Korea, November 16-17, 2006.
- Zhang, Y. (2008), "Piezoelectric paint sensors for ultrasonics-based damage detection", *Encyclopedia of Structural Health Monitoring*. Edited by C. Boller, F.-K. Chang and Y. Fujino, John Wiley & Sons, Ltd. ISBN: 978-0-470-05822-0.